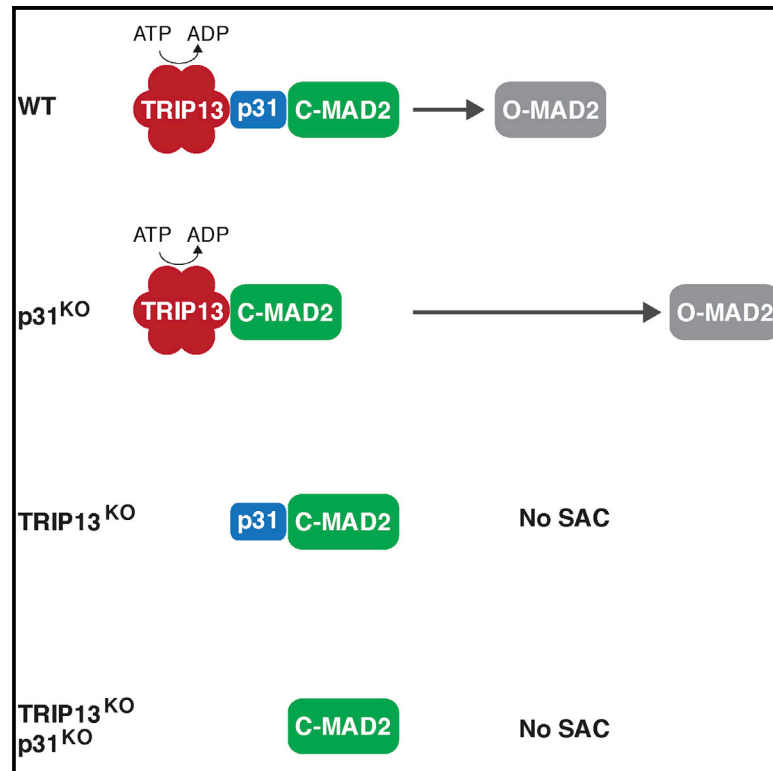# TRIP13 Regulates Both the Activation and Inactivation of the Spindle-Assembly Checkpoint

Graphical Abstract

Authors

Hoi Tang Ma, Randy Yat Choi Poon

Correspondence

rycpoon@ust.hk

In Brief

Mitotic exit requires the inactivation of MAD2. Ma and Poon show that MAD2 inactivation in mammalian cells requires TRIP13 and is stimulated by p31^{comet}. Moreover, TRIP13-deficient cells containing only C-MAD2 are unable to activate the spindle-assembly checkpoint.

Highlights

- Unperturbed mitosis is relatively normal in p31^{comet}- and TRIP13-deficient human cells

- MAD2 inactivation and mitotic exit are partially impaired without p31^{comet}

- TRIP13-deficient cells contain only C-MAD2

- TRIP13-deficient cells are unable to activate the spindle-assembly checkpoint

CrossMark

CellPress

Article

TRIP13 Regulates Both the Activation and Inactivation of the Spindle-Assembly Checkpoint

Hoi Tang Ma[1] and Randy Yat Choi Poon[1,*]

[1]Division of Life Science, Center for Cancer Research and State Key Laboratory of Molecular Neuroscience, The Hong Kong University of Science and Technology, Clear Water Bay, Hong Kong
*Correspondence: rycpoon@ust.hk

SUMMARY

Biochemical studies have indicated that p31^{comet} and TRIP13 are critical for inactivating MAD2. To address unequivocally whether p31^{comet} and TRIP13 are required for mitotic exit at the cellular level, their genes were ablated either individually or together in human cells. Neither p31^{comet} nor TRIP13 were absolutely required for unperturbed mitosis. MAD2 inactivation was only partially impaired in p31^{comet}-deficient cells. In contrast, TRIP13-deficient cells contained MAD2 exclusively in the C-MAD2 conformation. Our results indicate that although p31^{comet} enhanced TRIP13-mediated MAD2 conversion, it was not absolutely necessary for the process. Paradoxically, TRIP13-deficient cells were unable to activate the spindle-assembly checkpoint, revealing that cells lacking the ability to inactivate MAD2 were incapable in mounting a checkpoint response. These results establish a paradigm of the roles of p31^{comet} and TRIP13 in both checkpoint activation and inactivation.

INTRODUCTION

Mitotic exit is driven by a ubiquitin ligase called anaphase-promoting complex/cyclosome (APC/C) with its targeting subunit CDC20 (Pesin and Orr-Weaver, 2008). Unattached kinetochores or the absence of tension between the paired kinetochores activates the spindle-assembly checkpoint (SAC), which then prevents the activation of APC/C^{CDC20} (Musacchio, 2015). Hence, the SAC ensures that mitotic exit only occurs after all the chromosomes have achieved proper bipolar spindle attachment.

Components of the SAC include a diffusible MCC complex containing MAD2, BUBR1, BUB3, and CDC20, which facilitates the inhibition of APC/C^{CDC20} by MAD2. Binding to APC/C^{CDC20} requires a change in MAD2 from an open conformation (O-MAD2) to a more stable closed conformation (C-MAD2) (Yu, 2006). According to a generally accepted model, the C-MAD2 that binds to MAD1 at the kinetochores serves as a template for converting O-MAD2 into C-MAD2 (De Antoni et al., 2005). The C-MAD2 then forms the MCC, which in turns may serve as

a template for converting more O-MAD2 into C-MAD2. This model provides a mechanism for autoamplification and propagation of the SAC signal away from the kinetochores.

While significant progress has been made to unravel the underlying principles of SAC activation, lagging behind is our knowledge of how the SAC is turned off once the checkpoint is satisfied. Specifically, how C-MAD2 is converted back to O-MAD2 is a fundamental but outstanding question. There is compelling evidence that C-MAD2 is neutralized by binding to a protein called p31^{comet} (also called MAD2L1BP) in mammalian cells (Habu et al., 2002). For example, the SAC can be disrupted by p31^{comet} overexpression, and mitotic exit can be delayed by p31^{comet} knockdown (Habu et al., 2002; Xia et al., 2004; Chan et al., 2008a). Crystal structure of p31^{comet} reveals a folding similar to C-MAD2, suggesting that structural mimicry may be involved in checkpoint silencing (Yang et al., 2007).
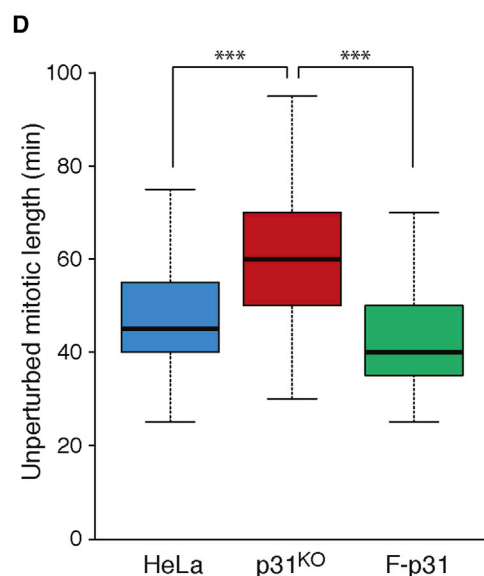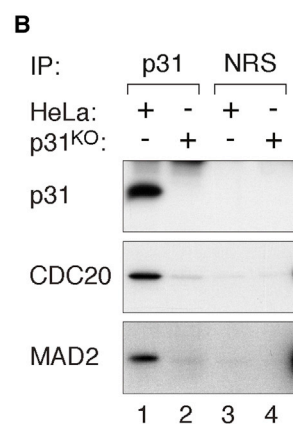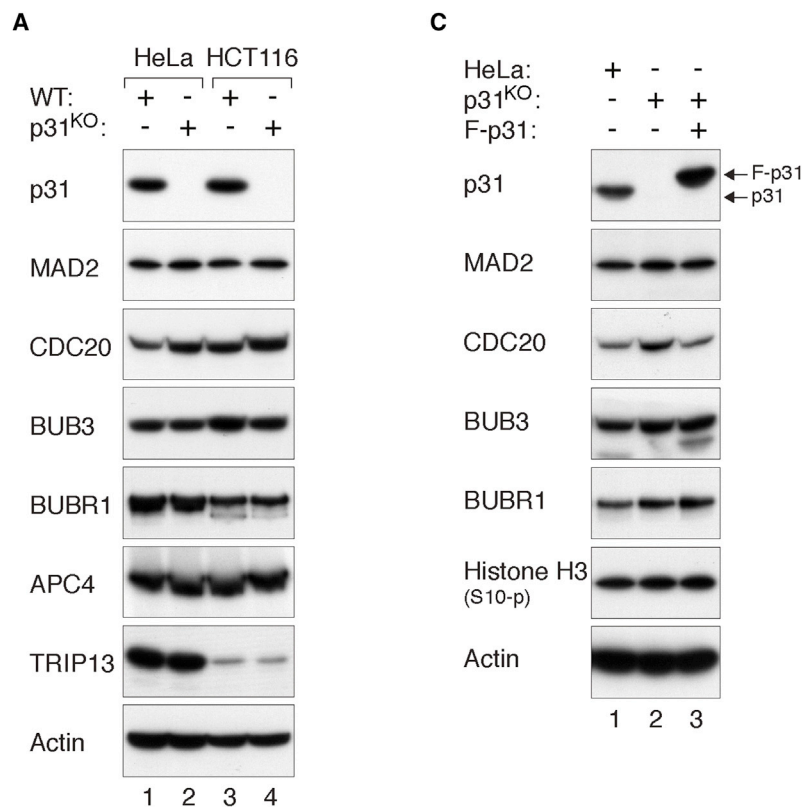
There is evidence that p31^{comet} is involved in the removal of MAD2 from MCC (Westhorpe et al., 2011). Disassembly of MCC by p31^{comet} is an ATP-dependent process, involving a p31^{comet}-interacting protein called TRIP13 (Eytan et al., 2014; Wang et al., 2014). TRIP13 is an AAA$^+$-ATPase that also functions in meiotic DNA break formation and recombination, checkpoint signaling, and chromosome synapsis (Vader, 2015). Recent structural and in vitro studies indicated that p31^{comet} acts both as an activator and an adaptor for TRIP13 for promoting C-MAD2 to O-MAD2 conversion (Ye et al., 2015). Whether p31^{comet} and TRIP13 are indeed responsible for MAD2 inactivation in the cell remains an important question.

In this study, we investigated the relative role of p31^{comet} and TRIP13 in SAC inactivation. We showed that both p31^{comet} and TRIP13 were not essential for unperturbed mitosis in different cell lines. We also found that C-MAD2 to O-MAD2 conversion was partially impaired in p31^{comet}-deficient cells and completely defective in TRIP13-deficient cells. Paradoxically, cells lacking TRIP13 displayed a relatively short mitosis and were unable to activate the SAC. We further demonstrate that direct binding of p31^{comet} to either MAD2 or TRIP13 was sufficient to promote mitotic exit.

RESULTS

p31^{comet} Is Not Essential for Unperturbed Mitosis

To address unequivocally whether p31^{comet} is required for mitotic exit, p31^{comet} gene (MAD2L1BP) was disrupted using TALEN (Figure S1A). Several clones of p31^{comet}-knockout

CrossMark

A

HeLa   HCT116

WT: +   -   +   -
p31^{KO}:   -   +   -   +

p31

MAD2

CDC20

BUB3

BUBR1

APC4

TRIP13

Actin

1   2   3   4

B

IP: p31   NRS

HeLa: +   -   +   -
p31^{KO}:   -   +   -   +

p31

CDC20

MAD2

1   2   3   4

C

HeLa: +   -   -
p31^{KO}:   -   +   +
F-p31:   -   -   +

p31   ← F-p31
    ← p31

MAD2

CDC20

BUB3

BUBR1

Histone H3
(S10-p)

Actin

1   2   3

D

Box-and-whisker plot. Y-axis: Unpopulated mitotic length (min), 0 to 100. Categories: HeLa, p31^{KO}, F-p31. *** significance markers between HeLa–p31^{KO} and p31^{KO}–F-p31.

Figure 1. p31^{comet} Is Not Essential for the Unperturbed Cell Cycle

(A) Ablation of p31^{comet} in HeLa and HCT116 cells. The p31^{comet} gene was disrupted in both HeLa and HCT116 cells using TALEN. The cells were synchronized in mitosis with NOC. Cell-free extracts were prepared, and the expression of p31^{comet} and related SAC components was analyzed with immunoblotting (p31^{KO}, p31^{comet} knockout). Equal loading of lysates was confirmed by immunoblotting for actin.

(B) Binding of MCC to p31^{comet} is disrupted in p31^{KO}. Mitotic extracts of WT and p31^{KO} HeLa cells prepared as in (A) were subjected to immunoprecipitation (IP) using an antiserum against p31^{comet} or normal rabbit serum (NRS). The immunoprecipitates were then analyzed using immunoblotting.

(C) Reintroduction of p31^{comet} to p31^{KO}. Parental HeLa, p31^{KO}, and p31^{KO} with stable expression of FLAG-p31^{comet} (F-p31) were synchronized and analyzed as in (A). The arrows indicated the positions of the endogenous and FLAG-tagged p31^{comet}.

(D) Knockout of p31^{comet} delays unperturbed mitotic progression. The indicated cell lines were infected with histone H2B-GFP-expressing retroviruses and analyzed with time-lapse fluorescence microscopy. Mitotic length of individual cells (from DNA condensation to anaphase onset) was determined and summarized in the box-and-whisker plot (n = 50). Deletion of p31^{comet} significantly extended the duration of mitosis and could be rescued with FLAG-p31^{comet} (***p < 0.001).

immunoprecipitates from p31^{KO} (Figure 1B). The p31^{comet} gene could also be ablated in HCT116 cells (Figure 1A), illustrating that the non-essential nature of p31^{comet} was not limited to one cell type.

The absence of p31^{comet} nevertheless led to abnormal mitosis. Time-lapse microscopy revealed that mitosis was significantly longer in p31^{KO} than in the parental HeLa (Figure 1D) or HCT116 cells (Figure S1C). To verify the causal relationship with p31^{comet}, recombinant FLAG-p31^{comet} was reintroduced into the p31^{KO} cells to a level comparable to the endogenous p31^{comet} before gene disruption (Figure 1C). The extension of mitosis caused by p31^{comet} knockout was completely reversed by the recombinant p31^{comet} (Figure 1D).

(p31^{KO}) cells were generated from HeLa (Figure S1B). Genomic DNA sequencing validated that deletions occurred at the TALEN-targeting region of *MAD2L1BP*, resulting in premature termination of the gene products (Figure S1A). Knockout of p31^{comet} did not alter the expression of MCC components, including MAD2, BUBR1, BUB3, and CDC20 (Figures 1A and S1A). As anticipated, no MAD2 or CDC20 was found in p31^{comet}

Taken together, these results indicate that although knockout of p31^{comet} delays mitotic exit, p31^{comet} is not essential for cells to complete mitosis.

Mitotic Exit Is Delayed in the Absence of p31^{comet}

We next analyzed whether p31^{comet} is important for prolonged mitotic arrest. Spindle poisons, including nocodazole (NOC),

activate the SAC and block cells in a prometaphase-like state. After washing out the NOC, the cells recovered rapidly from the checkpoint and undergo anaphase (Figure 2A, top). In contrast, mitotic exit was delayed by more than twofold in p31^{KO} cells, which could be reversed by reintroducing FLAG-p31^{comet}. Similar results were obtained using p31^{comet}-deficient HCT116 cells (Figure S1D). The delay of mitotic exit in p31^{KO} cells increased dramatically upon longer incubation in NOC (Figure 2A, middle), illustrating the importance of p31^{comet} for recovery after prolonged activation of the SAC.

The results from single-cell analysis were corroborated by other approaches, including the delays of the decrease of mitotic markers (histone H3^{Ser10} phosphorylation, cyclin B1, and CDC20) (Figure 2B) and cytokinesis (Figure 2C) after release from mitotic block. Mitotic exit eventually occurred after a delay of ~60 min (Figures 2D and 2E), again indicating that p31^{comet} is not absolutely required for checkpoint inactivation. Finally, timely mitotic exit was restored when p31^{comet} was reintroduced (Figures 2D and 2E).

Given that p31^{KO} cells required a longer time to recover from the SAC than p31^{comet}-containing cells, we predicted that p31^{KO} cells should be hypersensitive to spindle-disrupting agents. Indeed, a lower concentration of NOC was able to induce a mitotic delay in p31^{KO} than in parental HCT116 (Figure S1E).

The delay in mitotic exit in p31^{KO} was likely to be due to the time required for turning off the SAC. To test this hypothesis, cells were first released from NOC-mediated block into medium containing the proteasome inhibitor MG132—this trapped the cells in metaphase and satisfied the SAC—before finally released into drug-free medium. Using this method, anaphase onset was no longer delayed in p31^{KO} (Figure 2A, bottom).

An MPS1 inhibitor (MPS1i) was also used to abolish SAC activation. In normal cells, this triggered a rapid mitotic exit as indicated by cells containing G$_1$ DNA content (Figure S2A) and a decrease of mitotic markers (Figure S2B). In contrast, p31^{KO} cells entered G$_1$ only after a long delay following MPS1i treatment, again illustrating that p31^{comet} disruption affected SAC inactivation.

Collectively, these data demonstrate that after a delay, SAC inactivation and mitotic exit can occur in the absence of p31^{comet}.

p31^{comet} Is Partially Responsible for MAD2 Inactivation

Given that SAC inactivation involves C-MAD2 to O-MAD2 conversion, we next analyzed the conformation of MAD2 in the absence of p31^{comet}. A spin column-based ion exchange chromatography was adopted. O-MAD2 and C-MAD2 were eluted with relatively low and high salt concentrations, respectively (Figure 3A). Similar to endogenous MAD2, recombinant MAD2 was predominantly in the O-MAD2 conformation (Luo et al., 2004). A MAD2^{L13Q} mutant that only exists in the C-MAD2 conformation (Mapelli et al., 2007) eluted at relatively high salt concentration, verifying that the ion exchange chromatography was able to resolve the two forms of MAD2.

Consistent with previous studies (Luo et al., 2004), endogenous MAD2 was present predominantly as O-MAD2 (Figure 3B). We found that p31^{KO} contained more C-MAD2 than in control cells. As the total amount of MAD2 remain unchanged (Fig-

ure 3C), there was a net shift from O-MAD2 to C-MAD2 in the absence of p31^{comet}. Introduction of FLAG-p31^{comet} reversed this shift in MAD2 equilibrium. It is notable that C-MAD2 to O-MAD2 conversion was only partially impaired in p31^{KO} (compare with cells that were completely defective in this conversion below). An involvement of p31^{comet} in MAD2 inactivation was confirmed using an in vitro C-MAD2 to O-MAD2 conversion assay (see later).

Conceptually, a delay in SAC inactivation could be caused by a stimulation of MAD2 activation and/or a suppression of MAD2 inactivation. To see whether MAD2 activation is affected by p31^{comet}, the level of MCC was analyzed after the SAC was activated with NOC. The level of MAD2-CDC20 complexes increased after p31^{comet} was disrupted and could be reversed by FLAG-p31^{comet} (Figure 3C). Similarly, binding of MAD2 with other MCC components (BUBR1 and BUB3) increased in p31^{KO} cells (Figure S2C). Binding of APC4 (an APC/C subunit) to MCC also increased (p31^{comet} itself did not interact with APC4), indicating an enhancement of functional inhibition of APC/C after p31^{comet} was disrupted (Figure S2C).

Taken with the data below, these results demonstrate that p31^{comet} is involved in both suppressing MAD2 activation and inducing MAD2 inactivation.

### TRIP13 Is Essential for Converting MAD2 to the Open Conformation

Given that p31^{comet} is not absolutely required for SAC inactivation, we next addressed whether TRIP13, a recently identified partner of p31^{comet}, is essential for mitosis. We found that HeLa and HCT116 cells remained viable after the *TRIP13* gene was disrupted using CRISPR-Cas9 (Figure S3A). Interestingly, the expression of p31^{comet} was elevated in TRIP13^{KO} cells (Figure 4A; this is addressed later here).

In contrast to WT and p31^{KO} cells, TRIP13^{KO} contained MAD2 entirely in the C-MAD2 conformation (Figure 4B), suggesting that TRIP13 is required for converting C-MAD2 to O-MAD2 in the cell. Expression of a FLAG-TRIP13 construct restored the level of p31^{comet} (Figure 4C) as well as the C-MAD2 to O-MAD2 equilibrium (Figure 4D).

To further validate the essential role of TRIP13 in C-MAD2 to O-MAD2 conversion, we developed an in vitro MAD2 conversion assay. Lysates of TRIP13^{KO} cells were supplemented with an ATP-regeneration system and incubated for 90 min (Figure 4E). During this time, the MAD2 in the TRIP13^{KO} lysates remained in the C-MAD2 conformation. Mixing in a small portion of HeLa cell lysates (10:1 ratio) was sufficient to convert the C-MAD2 in the TRIP13^{KO} lysates into O-MAD2. Moreover, addition of bacterially expressed GST-TRIP13 was also sufficient to convert the C-MAD2 into O-MAD2 in vitro (Figure 4F).

Consistent with the high levels of p31^{comet} and C-MAD2 in TRIP13^{KO}, there was a corresponding increase in p31^{comet}-MAD2 complexes (despite the fact that the expression of total MAD2 was reduced) (Figure 4G). Dissociation of these p31^{comet}-MAD2 complexes was promoted by mixing of TRIP13-containing lysates (Figure 4H).

Given that MAD1 was eluted at similar fractions as C-MAD2 in ion exchange chromatography (Figure S3B), it is possible that the shift of MAD2 to high-salt fractions in TRIP13^{KO} was simply
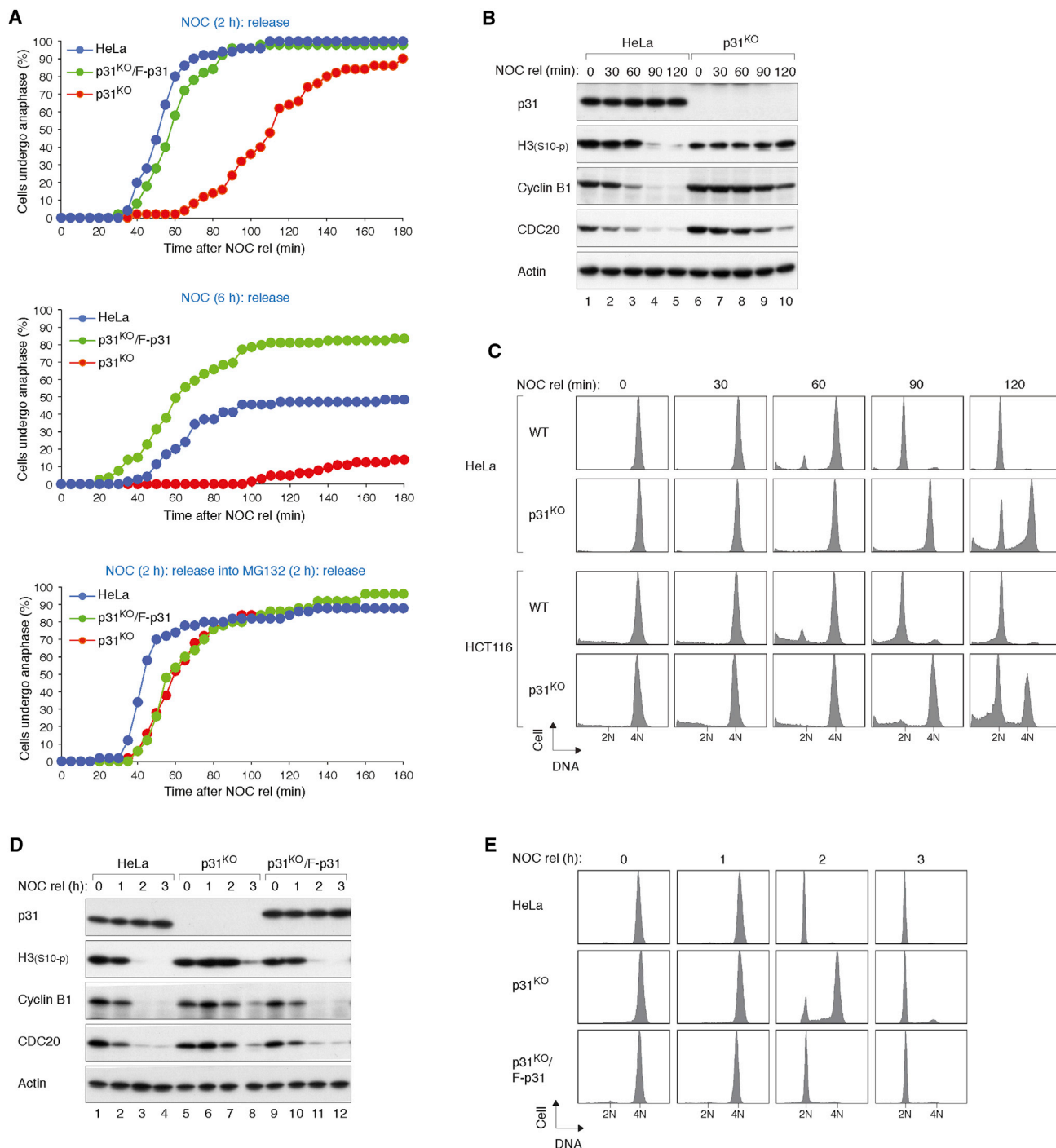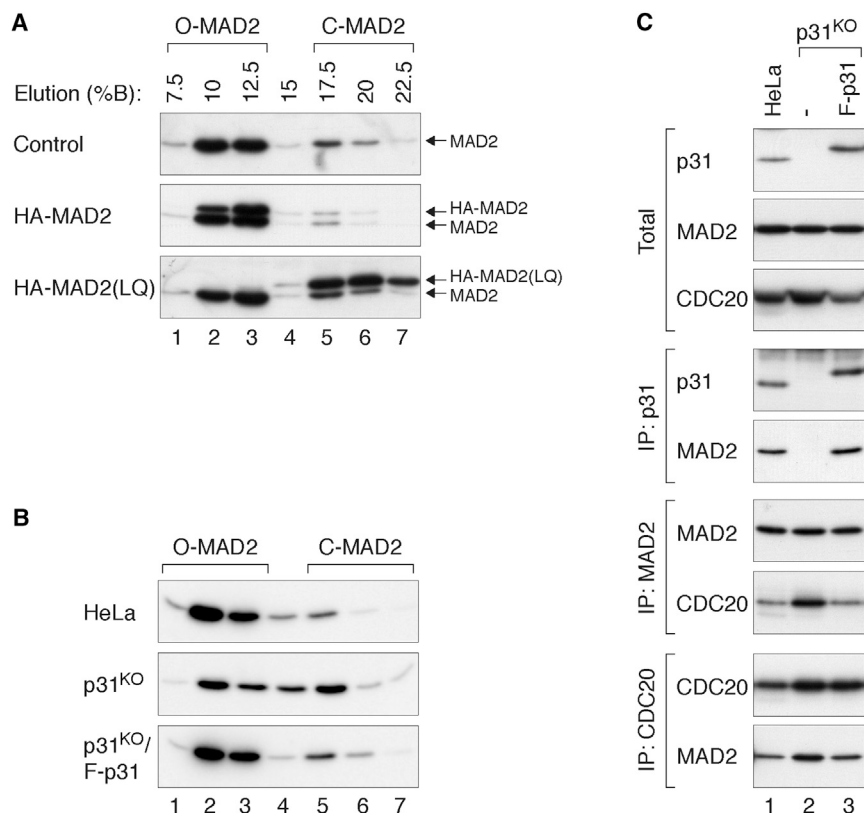
Figure 2. p31^comet Is Important for Mitotic Exit after Prolonged SAC Activation

(A) Mitotic exit is delayed in p31^comet-deficient cells. Histone H2B-GPF-expressing HeLa, p31^KO, and p31^KO expressing FLAG-p31^comet (F-p31) were synchronized in mitosis with NOC (2 hr) followed with mechanical shake-off. (Top) The cells were washed twice with PBS and released into drug-free medium. The cells were imaged immediately with time-lapse microscopy, and mitotic progression was analyzed. (Middle) The mitotic cells were further incubated in NOC-containing medium for another 4 hr before releasing and imaging. (Bottom) Cells were prepared as in the top, except that they were first released into MG132-containing medium (2 hr) before released into drug-free medium for imaging.

(B) Mitotic exit is delayed in p31^comet-deficient cells. HeLa and p31^KO were synchronized in mitosis with NOC. The cells were then released into NOC-free medium and harvested at the indicated time points. Lysates were prepared, and the expression of the indicated proteins was analyzed with immunoblotting. Mitotic exit was indicated by the decrease of histone H3^Ser10 phosphorylation, cyclin B1, and CDC20.

(legend continued on next page)

A

O-MAD2   C-MAD2

Elution (%B): 7.5 10 12.5 15 17.5 20 22.5

Control — ← MAD2

HA-MAD2 — ← HA-MAD2 / ← MAD2

HA-MAD2(LQ) — ← HA-MAD2(LQ) / ← MAD2

1 2 3 4 5 6 7

B

O-MAD2   C-MAD2

HeLa

p31^{KO}

p31^{KO}/ F-p31

1 2 3 4 5 6 7

C

p31^{KO}

HeLa − F-p31

Total:
p31
MAD2
CDC20

IP: p31:
p31
MAD2

IP: MAD2:
MAD2
CDC20

IP: CDC20:
CDC20
MAD2

1 2 3

Figure 3. p31^{comet} Facilitates the Maintenance of MAD2 in the Open Conformation

(A) MAD2 is mainly present in the O-MAD2 conformation in the cell. Control HeLa or cells transfected with plasmids expressing HA-tagged MAD2 or a C-MAD2-specific mutant (MAD2(LQ)) were analyzed using spin column-based ion exchange chromatography. Fractions were eluted with different concentrations of buffer B (%B, Experimental Procedures) and analyzed with immunoblotting for MAD2. The fractions corresponding to O-MAD2 and C-MAD2 are indicated at the top. The positions of the endogenous and recombinant MAD2 are indicated.

(B) C-MAD2 to O-MAD2 conversion is partially impaired in the absence of p31^{comet}. MAD2 conformation in HeLa cells, p31^{KO}, and p31^{KO} expressing FLAG-p31^{comet} was analyzed with ion exchange chromatography.

(C) Knockout of p31^{comet} induces an accumulation of MCC. The indicated cell lines were enriched in mitosis with NOC. Lysates were prepared and subjected to immunoprecipitation using antiserum against p31^{comet}, MAD2, or CDCD20. The immunoprecipitates and total lysates were then analyzed using immunoblotting.

due to an increase in MAD2-MAD1 complexes. In disagreement with this, MAD2-MAD1 complexes were present at similar levels in HeLa and TRIP13^{KO} cells (Figure S3C). Removal of MAD1 from TRIP13^{KO} lysates by immunodepletion only slightly reduces the total MAD2 (Figure S3D). Furthermore, MAD2 was still eluted at high-salt fractions after MAD1 was depleted (Figure S3E).

Collectively, our data indicate that TRIP13 is required for converting C-MAD2 into O-MAD2.

Loss of TRIP13 Disrupts the SAC

Given that TRIP13 is required for C-MAD2 into O-MAD2 conversion, we predicted that TRIP13-deficient cells are unable to inactivate the SAC to induce mitotic exit. Accumulation and decrease of mitotic histone H3^{Ser10} phosphorylation occurred relatively normally in synchronized TRIP13^{KO} (Figure 5A), indicating that unperturbed mitosis was unaffected by the absence of TRIP13. Live-cell imaging further detailed that TRIP13^{KO} could undergo mitosis relatively normally (albeit shorter than in normal cells, see Figure 6B).

In complete opposite to our expectation, TRIP13^{KO} cells were unable to be trapped in mitosis with NOC (Figure 5B). Compared

with control cells, histone H3^{Ser10} phosphorylation increased only transiently, suggesting that the SAC either could not be activated properly or be maintained in the absence of TRIP13. Similar results were obtained from multiple clones of TRIP13^{KO} cells in both HeLa (Figure S4A) and HCT116 background (Figure S4B).

Time-lapse microscopy was further used to verify that TRIP13 is required for maintaining the SAC at the single-cell level. While control NOC-treated HeLa cells remained in mitosis for ~10 hr before undergoing slippage, TRIP13^{KO} cells underwent slippage in less than 1 hr (Figure 5C). The SAC could be restored with recombinant TRIP13, supporting a causal relationship between TRIP13 inactivation and the loss of the checkpoint. As a control, expression of TRIP13 alone did not affect the duration of mitotic arrest in HeLa cells.

TRIP13-rescue experiments were also performed to analyze histone H3^{Ser10} phosphorylation. While exposing HeLa cells to NOC induced an accumulation of histone H3^{Ser10} phosphorylation, no phosphorylation was detected using TRIP13^{KO} (Figure 5D). Histone H3^{Ser10} phosphorylation was also analyzed in individual cells using flow cytometry (Figure 5E). In both assays, the deficiency in NOC-induced histone H3^{Ser10} phosphorylation could be rescued with recombinant TRIP13. The SAC was not restored with a TRIP13 Walker-A domain mutant,

(C) Delayed entry into G$_1$ in the absence of p31^{comet}. HeLa and HCT116 (both WT and p31^{KO}) were blocked in mitosis with NOC and released as in (B). The cells were fixed at the indicated time points and analyzed with flow cytometry. The positions of 2N (G$_1$) and 4N (G$_2$/M) DNA contents are indicated.

(D) Delayed disappearance of mitotic markers in p31^{comet}-deficient cells. HeLa, p31^{KO}, and p31^{KO} expressing FLAG-p31^{comet} were synchronized in mitosis with NOC. The cells were then released into NOC-free medium and harvested at the indicated time points. Lysates were prepared and analyzed with immunoblotting.

(E) Entry into G$_1$ from mitotic arrest is delayed without p31^{comet}. Different cells were released from mitotic block as in (D). The cells were fixed at the indicated time points and analyzed with flow cytometry.
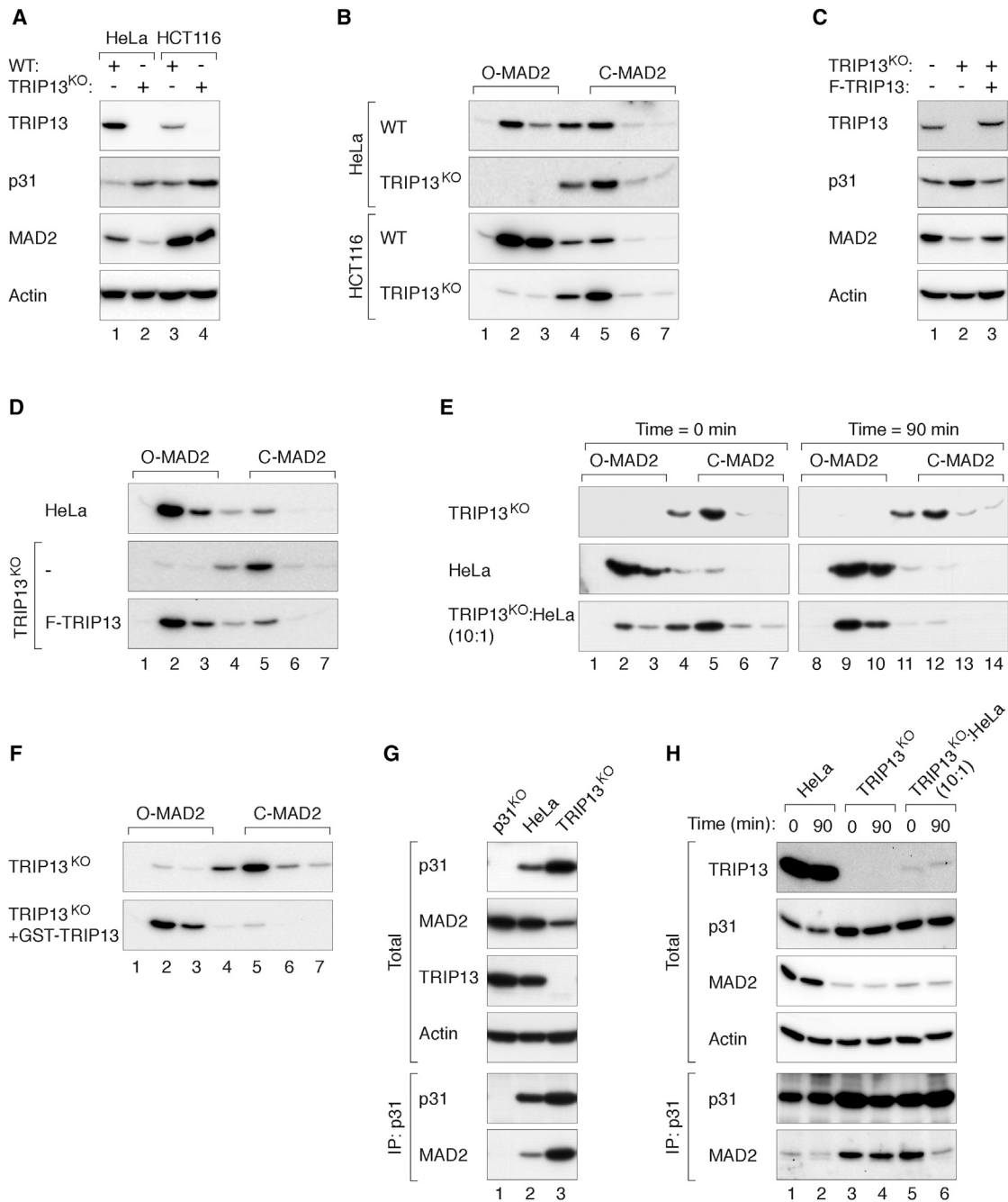
Figure 4. TRIP13 Is Essential for Converting MAD2 to the Open Conformation

(A) Disruption of TRIP13 in HeLa and HCT116 cells. *TRIP13* gene was disrupted in both HeLa and HCT116 cells using CRISPR-Cas9 (TRIP13^{KO}, TRIP13 knockout). Lysates were prepared, and the expression of TRIP13 and other proteins was analyzed with immunoblotting (note that 10 μg was loaded for HeLa and 20 μg was loaded for HCT116).

(B) C-MAD2 to O-MAD2 conversion requires TRIP13. MAD2 conformation in parental HeLa or HCT116 and the corresponding TRIP13^{KO} cells was analyzed using ion exchange chromatography.

(C) An increase in p31^{comet} after TRIP13 disruption can be reversed by recombinant TRIP13. Lysates of HeLa, TRIP13^{KO}, or TRIP13^{KO} infected with retroviruses producing FLAG-TRIP13 were analyzed with immunoblotting.

(D) Recombinant TRIP13 restores C-MAD2 to O-MAD2 conversion in TRIP13^{KO}. MAD2 conformation in parental HeLa, TRIP13^{KO}, or TRIP13^{KO} infected with retroviruses producing FLAG-TRIP13 was analyzed with ion exchange chromatography.

(E) TRIP13-dependent C-MAD2 to O-MAD2 conversion in cell lysates. Lysates of HeLa or TRIP13^{KO} were supplemented with an ATP-regeneration system and incubated at 25°C. A third reaction included mixing of TRIP13^{KO} and HeLa lysates at a 10:1 ratio. At the indicated time points, the reactions were stopped, and MAD2 conformation was analyzed.

(legend continued on next page)

which abolishes the ATPase activity (Hanson and Whiteheart, 2005), indicating that SAC functions requires the presence of catalytic-active TRIP13 (Figure 5F).

MAD2 was enriched at the kinetochores of both HeLa and TRIP13^{KO} mitotic cells (Figure S4C). This indicated that the lack of SAC was not due to aberrant MAD2 recruitment and suggested that downstream activation of MCC may be dysregulated in TRIP13^{KO}. Since TRIP13^{KO} could not be trapped in mitosis by conventional methods, we first synchronized the cells to G$_2$ using a CDK1 inhibitor before releasing them into NOC. A proteasome inhibitor (MG132) was added to prevent the TRIP13^{KO} cells from escaping mitosis. Figure 5G shows that TRIP13^{KO} contained less MCC than control cells, again supporting the idea that TRIP13 is required for the SAC activation.

As the expression of total MAD2 decreased in TRIP13^{KO} cells (Figure 4C), we also examined the effects of MAD2 expression on the SAC. While the SAC in TRIP13^{KO} cells could be restored by TRIP13, it remained defective after ectopic expression of MAD2 (Figure S4D), indicating that the defective SAC in TRIP13^{KO} cells was not caused by a decrease in MAD2.

Hence, paradoxically, instead of delayed SAC inactivation, disruption of TRIP13 resulted in defective activation of the SAC. Although exclusively C-MAD2 was present in these cells, it was unable to be incorporated into MCC to establish the checkpoint.

p31^{comet} Promotes TRIP13-Dependent C-MAD2 to O-MAD2 Inactivation

One trivial explanation of the lack of SAC in TRIP13^{KO} is the increase of p31^{comet} in these cells (Figures 4A and 5D). To test this possibility, we first depleted p31^{comet} with siRNA and demonstrated that TRIP13^{KO} cells were still without SAC (Figure S4E). We further generated cells lacking both TRIP13 and p31^{comet} together (Figure 6A). During unperturbed cell cycle, TRIP13^{KO} cells already displayed a relatively short mitosis (Figure 6B). This was not caused by changes in p31^{comet} because the mitotic length was not restored in the double-knockout cells. Similar to cells lacking TRIP13 alone, cells lacking both TRIP13 and p31^{comet} together were defective in SAC activation, as revealed by histone H3^{Ser10} phosphorylation (Figure 6C) and mitotic length analysis (Figure 6D). Furthermore, similar to TRIP13^{KO} (Figure 4B), the double-knockout cells contained mainly C-MAD2 (Figure 6E).

Collectively, these data indicated that the defects in SAC activation and MAD2 conversion in TRIP13^{KO} were independent on p31^{comet}. In fact, expressing FLAG-TRIP13 in TRIP13^{KO}/p31^{KO} double-knockout cells was sufficient to reestablish the C- to O-MAD2 equilibrium (Figures 6A and 6E). Nevertheless, p31^{comet}

was involved in facilitating TRIP13-dependent MAD2 conversion. Addition of purified GST-TRIP13 to TRIP13-deficient lysates effectively converted C-MAD2 to O-MAD2 (Figure 6F). In contrast, MAD2 conversion was significantly slower in lysates that also lacked p31^{comet}. These data indicated that p31^{comet} increases the efficiency of TRIP13-dependent MAD2 inactivation.

Taken together, these data reveal that although p31^{comet} accumulates in TRIP13^{KO}, it is not responsible for the defective SAC activation in these cells. TRIP13 is required for the conversion of C-MAD2 to O-MAD2, a process that is promoted by p31^{comet}.

Interaction of p31^{comet} with Either MAD2 or TRIP13 Can Promote Mitotic Exit

Recent in vitro studies indicated that p31^{comet} acts both as an adaptor between MAD2 and TRIP13 as well as an activator of TRIP13 (Ye et al., 2015). As our data showed that MAD2 could still be inactivated in the absence of p31^{comet}, we next examined the interaction between MAD2, TRIP13, and p31^{comet} in the cell. Co-immunoprecipitation analysis indicated that both MAD2 and p31^{comet} could interact with TRIP13 (Figure 7A). Significantly, MAD2 also co-immunoprecipitated with TRIP13 in a p31^{comet}-deficient background, suggesting the possibility of a direct TRIP13-MAD2 interaction (Figure 7B).

To understand how p31^{comet} promoted TRIP13-dependent MAD2 inactivation, we generated a Q83A/F191A mutant of p31^{comet} (p31(QF) herein) that cannot bind MAD2 (Yang et al., 2007). Figure S5A confirms that p31(QF) did not interact with MAD2. To test whether interaction with TRIP13 is important for p31^{comet}'s function, we further generated a mutant of p31^{comet} that disrupted binding to TRIP13 (P228A/K229A, Ye et al., 2015, p31(PK) herein). Figure S5B shows that while p31^{comet} bound robustly to an ATPase-inactive mutant of TRIP13 (which forms stable hexamers, Ye et al., 2015, and trapped p31^{comet} better than WT TRIP13 in our assays), this interaction was abolished in p31(PK).

As shown above, TRIP13^{KO} cell lysates contained predominantly C-MAD2, which could be converted into O-MAD2 with GST-TRIP13 in a p31^{comet}-dependent manner (Figure 7C). In contrast, the non-MAD2 binding p31(QF) did not promote MAD2 conversion. The non-TRIP13 binding p31(PK) was also impaired in inducing MAD2 conversion in vitro (but was marginally more efficient than p31(QF)). In agreement with these results, the accumulation of MCC in p31^{KO} could be rescued with p31^{comet}, p31(PK), but not p31(QF) (Figure 7D). Figure 7E indicates that all the p31^{comet} constructs were expressed at levels comparable to endogenous p31^{comet}.

(F) Bacterially expressed TRIP13 stimulates C-MAD2 to O-MAD2 conversion in lysates. Lysates of TRIP13^{KO} were supplemented with an ATP-regeneration system and incubated in either the presence or absence of bacterially expressed GST-TRIP13. After 45 min, the reactions were stopped, and MAD2 conformation was analyzed.

(G) Increased level of p31^{comet}-MAD2 complexes in TRIP13^{KO}. Lysates of HeLa, p31^{KO}, and TRIP13^{KO} were subjected to immunoprecipitation using antiserum against p31^{comet}. The expression of the indicated proteins in total lysates and p31^{comet}-immunoprecipitates was analyzed with immunoblotting.

(H) TRIP13 stimulates the dissociation of p31^{comet}-MAD2 complexes. Lysates of HeLa, TRIP13^{KO}, or a mixture of TRIP13^{KO} lysates with HeLa lysates (10:1) were supplemented with an ATP-regeneration system and incubated at 25°C. The cells were harvested at the indicated time points. Lysates were prepared and subjected to immunoprecipitation using antiserum against p31^{comet}. The expression of the indicated proteins in total lysates and p31^{comet}-immunoprecipitates was analyzed with immunoblotting.
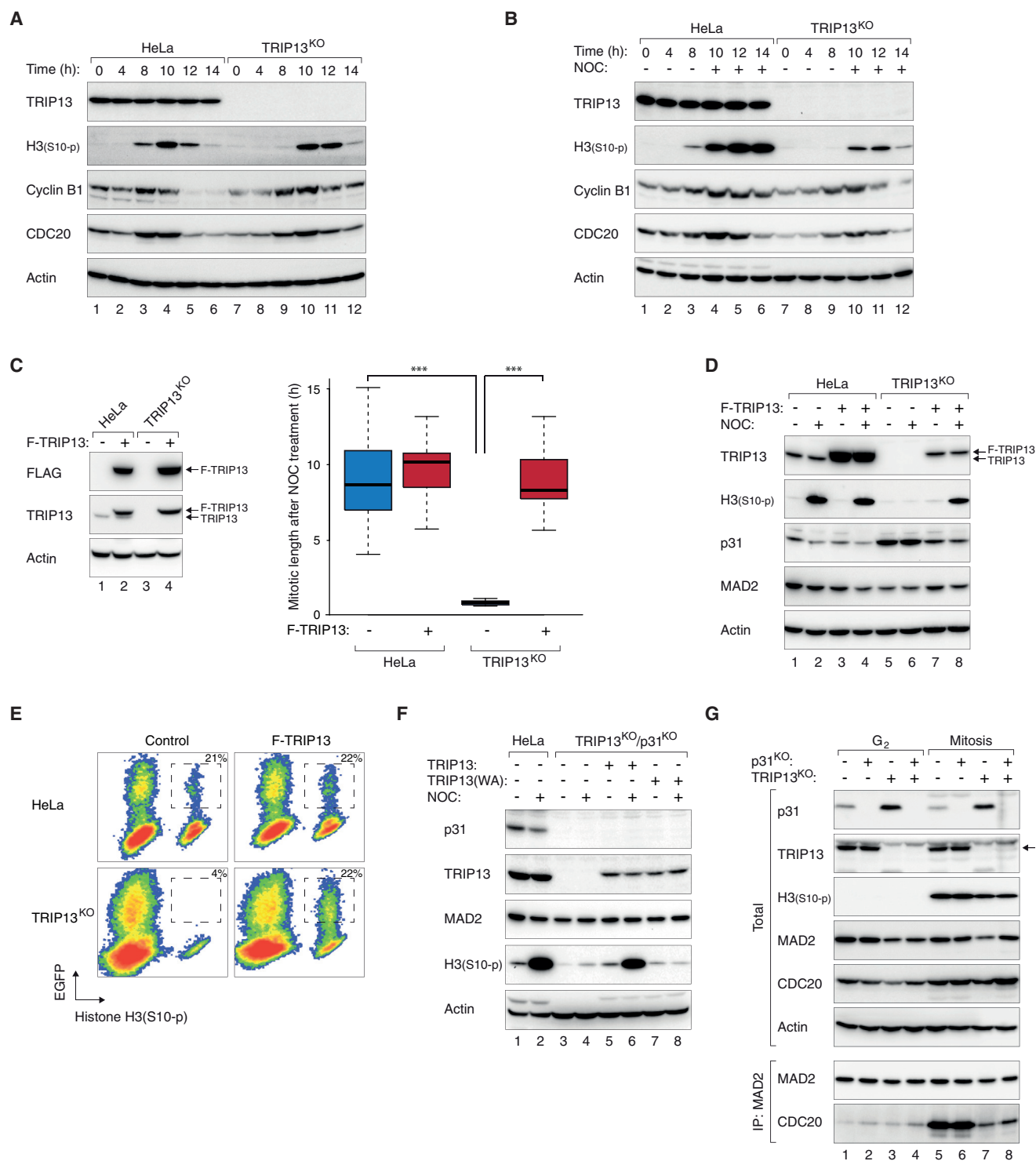
Figure 5. TRIP13 Is Essential for the Activation of the SAC

(A) TRIP13 is not required for unperturbed mitosis. HeLa and TRIP13[KO] were synchronized at early S phase with a double thymidine procedure and released into the cell cycle. The cells were harvested at the indicated time points and analyzed with immunoblotting.

(B) TRIP13-deficient cells are unable to maintain a mitotic arrest. HeLa and TRIP13[KO] were synchronized at early S phase with a double thymidine procedure and released into the cell cycle in the presence of NOC. The cells were harvested at the indicated time points and analyzed with immunoblotting.

(C) TRIP13 is required for prolonged mitotic arrest. HeLa and TRIP13[KO] were infected with FLAG-TRIP13-expressing retroviruses. Lysates were produced and analyzed with immunoblotting (upper). The cells were also incubated with NOC and analyzed with time-lapse fluorescence microscopy. The mitotic length of

Although both p31(QF) and p31(PK) have relatively weak MAD2-inactivating activity in vitro, cells expressing them were able to enter G_1 with the same kinetics as cells expressing WT p31^{comet} (Figure 7E). In contrast, p31^{comet} that could bind neither MAD2 nor TRIP13 (p31(QF/PK)) (Figures S5A and S5C) were unable to rescue the mitotic exit delay caused by p31^{comet} knockout (Figure 7F). Not surprisingly, p31(QF/PK) was also unable to promote C-MAD2 to O-MAD2 conversion in vitro (Figure 7C) or MCC inactivation (Figure 7G). Finally, compared with cells expressing p31(QF) or p31(PK), p31(QF/PK)-expressing cells displayed an impaired MAD2 equilibrium similar to cells without any p31^{comet} (Figure 7H).

Taken together, these results indicated that although direct binding of p31^{comet} to both MAD2 and TRIP13 is important for facilitating TRIP13-dependent MAD2 inactivation in vitro, p31^{comet} mutants that lack either one of these functions appear to be sufficient to promote mitotic exit.

DISCUSSION

Existing evidence predicts that p31^{comet} and TRIP13 are essential for mitosis. However, our results indicate that both proteins are not essential proteins for the unperturbed cell cycle. The conclusion was based on evidence from gene disruption in two different cell lines. Given that both inactivation and activation of SAC were affected in p31^{KO} and TRIP13^{KO}, respectively, deficiencies of the SAC appear to be well tolerated during unperturbed mitosis. It should be noted that mitosis was actually delayed in p31^{comet}-deficient cells (Figures 1D and S1C) and shortened in TRIP13-deficient cells (Figure 6D). However, these defects did not appear to compromise cell survival in both HeLa and the more chromosomally stable HCT116. An implication is that an effective SAC is not absolutely necessary for cell survival, at least in the cell lines examined. As the use of the same gene-editing tools is challenging in cells with finite proliferation potential, it is currently unclear whether the same is also true for normal cells. In this connection, *Trip13*-deficient mice (generated with gene-trap techniques and contained vastly reduced level of Trip13) are born at approximately two-thirds the expected ratio but are otherwise grossly normal (Li and Schimenti, 2007).

The delay in mitotic exit in the absence of p31^{comet} (Figure 2) correlated with an increase in MCC (Figures 3C and S2C), suggesting that p31^{comet} might antagonize MAD2 activation. Disruption of p31^{comet} also prevented TRIP13-dependent MAD2 inactivation in vitro (Figure 6F), indicating a role of p31^{comet} in MAD2 inactivation. This notion is also supported by the shift of C-MAD2 and O-MAD2 equilibrium in p31^{KO} (Figure 3B). Hence, a combination of a higher level of MCC attained during SAC activation and a slower rate of MAD2 inactivation after the SAC was satisfied contributed to the delay in mitotic exit in p31^{KO}.

One of the surprising findings from this study is that mitotic exit could occur in p31^{KO}, albeit at a slower rate than p31^{comet}-containing cells (Figure 2). Likewise, in vitro MAD2 inactivation could occur in a p31^{comet}-deficient background (Figure 6F). These results are consistent with the model that TRIP13-dependent MAD2 inactivation can occur in the absence of p31^{comet}. Given that TRIP13 could associate with MAD2 without p31^{comet} (Figure 7B), it is possible that MAD2 inactivation could occur at a relatively slow rate without p31^{comet}. These results deviate from previous yeast three-hybrid and in vitro studies, in which the interaction between TRIP13 and MAD2 is dependent on the presence of p31^{comet} (Ye et al., 2015). Ye et al. (2015) proposed a two-states binding model in which MAD2 first binds TRIP13 through a transient TRIP13-p31^{comet} interaction followed by a direct interaction between TRIP13 and MAD2. Our results suggested that TRIP13-p31^{comet}-MAD2 might not be absolutely required for TRIP13 to act on MAD2.

We found that mitotic exit could be promoted by p31(QF), a mutant that cannot bind MAD2 (Figure 7E). Hence, it is possible that although p31(QF)-expressing cells contained elevated levels of MCC (Figure 7D), the stimulation of TRIP13 activity by p31^{comet} was sufficient to promote mitotic exit. However, the non-TRIP13 binding p31(PK) also facilitated mitotic exit (Figure 7E). It is possible that p31(PK) was able to make MAD2 a better substrate for TRIP13. In agreement with this, both p31(QF) and p31(PK) were able to stimulate TRIP13-dependent MAD2 inactivation (Figure 7H). In contrast, p31^{comet} that bound neither MAD2 nor TRIP13 was unable to promote mitotic exit (Figure 7F) or MAD2 inactivation (Figure 7H). It is important to note that we cannot exclude the possibility that p31(PK) or p31(QF) could still interact weakly or transiently with TRIP13 or MAD2, respectively. However, our available data indicate that even with a Walker B mutant of TRIP13 (which probably acts as a substrate trap for p31^{comet}-MAD2), no p31(PK) was detected to form a complex (Figure S5B).

Although TRIP13 is responsible for inactivating the SAC, TRIP13^{KO} cells were unable to activate the SAC (Figures 5B–5E). In agreement with this, a *C. elegans* TRIP13 (PCH-2) mutant

individual cells was determined (from DNA condensation to slippage or cell death) (n = 50) (lower). Deletion of TRIP13 abolished mitotic arrest and could be rescued with TRIP13 (***$p < 0.001$).

(D) Recombinant TRIP13 reestablishes the SAC in TRIP13-deficient cells. HeLa and TRIP13^{KO} were transfected with FLAG-TRIP13-expressing plasmids. The cells were then incubated with either buffer or NOC for 16 hr before analyzed with immunoblotting.

(E) Recombinant TRIP13 restores histone H3^{Ser10} phosphorylation in TRIP13-deficient cells. HeLa and TRIP13^{KO} were transfected with FLAG-TRIP13-expressing plasmids. EGFP-expressing plasmids were co-transfected as markers. The cells were then incubated with NOC for 6 hr. The portion of phosphor-histone H3^{Ser10}- and EGFP-positive cells was analyzed by bivariate flow cytometry.

(F) ATP hydrolase activity of TRIP13 is required for restoring the SAC in TRIP13-deficient cells. HeLa and TRIP13^{KO} were transfected with plasmids expressing TRIP13 or TRIP13(WA) mutant. The cells were then incubated with either buffer or NOC for 16 hr before analyzed with immunoblotting.

(G) Defective MCC formation in the absence of TRIP13. HeLa, p31^{KO}, TRIP13^{KO}, or double-knockout cells were released from double thymidine block. After 7 hr, the cells were incubated with the CDK1 inhibitor RO3306 for 5 hr to trap cells in G_2. After washing out the RO3306 (30 min), the cells were incubated with NOC and MG132 for 2 hr to enrich cells in mitosis (as indicated by histone H3^{Ser10} phosphorylation). Lysates were prepared and subjected to immunoprecipitation using an antibody against MAD2. Both the total lysates and the immunoprecipitates were analyzed with immunoblotting.
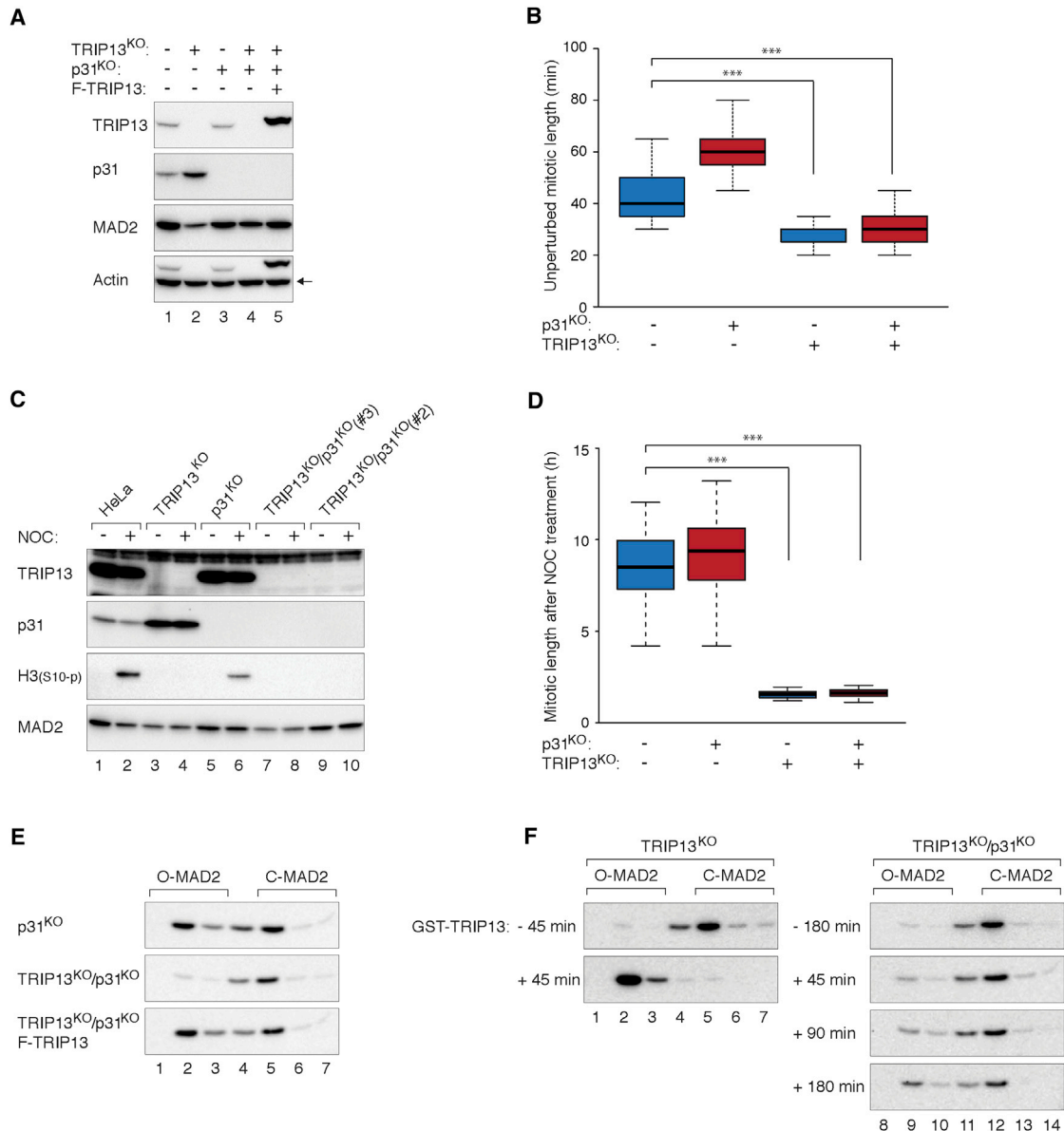
Figure 6. Inactivation of p31[comet] Is Not Sufficient to Restore the SAC in TRIP13 Knockout Cells

(A) Ablation of both TRIP13 and p31[comet]. Lysates from cells lacking TRIP13 and p31[comet], either individually or together, were analyzed with immunoblotting. Lysates from TRIP13[KO]/p31[KO] expressing FLAG-TRIP13 was also loaded. Equal loading of lysates was confirmed by immunoblotting for actin (the upper bands were signals from the TRIP13 blot).

(B) The shortening of unperturbed mitosis in TRIP13[KO] cannot be rescued with co-knockout of p31[comet]. The indicated cell lines were infected with histone H2B-GFP-expressing retroviruses and analyzed with time-lapse microscopy. The mitotic length of individual cells was determined (n = 50). Mitosis was significantly shortened after deletion of TRIP13 or both TRIP13 and p31[comet] together (***p < 0.001).

(C) Removal of p31[comet] cannot restore the SAC in TRIP13[KO]. The indicated cell lines (including two different clones of TRIP13[KO]/p31[KO]) were incubated with either buffer or NOC for 16 hr before analyzed with immunoblotting.

(D) Removal of p31[comet] cannot restore the SAC in TRIP13[KO]. The indicated cell lines were infected with histone H2B-GFP-expressing retroviruses, incubated with NOC, and analyzed with time-lapse microscopy. The mitotic length of individual cells was determined (n = 50). Mitotic arrest was significantly shortened after deletion of TRIP13 or TRIP13 and p31[comet] together (***p < 0.001).

(E) Defective C-MAD2 to O-MAD2 conversion in TRIP13[KO] cannot be rescued by removing p31[comet]. MAD2 conformation in p31[KO], TRIP13[KO]/p31[KO], or TRIP13[KO]/p31[KO] infected with retroviruses producing FLAG-TRIP13 was analyzed with ion exchange chromatography.

(F) Efficient TRIP13-dependent C-MAD2 to O-MAD2 conversion requires p31[comet]. Lysates of TRIP13[KO] or TRIP13[KO]/p31[KO] were supplemented with an ATP-regeneration system and incubated in either the presence or absence of bacterially expressed GST-TRIP13. At the indicated time points, the reactions were stopped, and MAD2 conformation was analyzed with ion exchange chromatography.

was also found to be defective in SAC activation (Nelson et al., 2015). This unexpected result may be reconciled by the fact that MAD2 equilibrium was disrupted (Figure 4B). Although TRIP13-deficient cells contained exclusively C-MAD2, the C-MAD2 was unable to be incorporated into MCC (Figure 5G). The normal localization of MAD2 to the kinetochores (Figure S4C) and MAD2-MAD1 complex formation (Figure S3C) suggested that perhaps the propagation of the MAD2 signal to the MCC was affected without TRIP13. One possibility is that the activation of the SAC may require dynamic conversion of C-MAD2 from O-MAD2, rather than simply the presence of C-MAD2 itself. These are provocative ideas that will need to be tested in the future, for example, by replacing the endogenous MAD2 with a C-MAD2-specific mutant.

The fact that TRIP13^{KO} cells were unable to be enriched in mitosis presented a difficulty for studying the role of TRIP13 in SAC inactivation. Nevertheless, by using an in vitro MAD2 conversion assay, we demonstrated that TRIP13 could induce C-MAD2 to O-MAD2 conversion, particularly in a p31^{comet}-containing environment (Figure 6F). In another approach using G$_2$ synchronization and a proteasome inhibitor, we demonstrated that MCC formation was defective without TRIP13 (Figure 5G). These data are consistent with previous RNAi experiments showing that depletion of TRIP13 results in a delay in mitotic exit in MCF7 cells (Wang et al., 2014). However, our results are inconsistent with these previous experiments in one important aspect. While Wang et al. (2014) showed that knockdown of TRIP13 inhibits cell proliferation in breast cancer cell lines, our gene-disruption studies showed that both HeLa and HCT116 cells could survive without TRIP13. A more elegant demonstration of a role of TRIP13 in SAC inactivation will involve approaches that allow us to inactivate TRIP13 rapidly during a mitotic block.

Loss of TRIP13 was associated with an accumulation of p31^{comet} and a decrease in MAD2. They were unlikely to be off-target effects because they could be reversed with a recombinant TRIP13 (Figure 4C). Although these changes in p31^{comet} and MAD2 were not responsible for the SAC defects in TRIP13-deficient cells (Figures 6C, 6D, and S4D), it is nevertheless an interesting phenomenon that may be inextricably linked to the SAC. One possible explanation is that the accumulation of C-MAD2 caused by TRIP13-knockout could stabilize p31^{comet}.

As the expression of TRIP13 affects SAC activation, a prediction from this study is that TRIP13 should be tightly regulated to prevent genome instability. *TRIP13* gene is amplified or its product is overexpressed in several cancers (Rhodes et al., 2004; Banerjee et al., 2014; Larkin et al., 2012; van Kester et al., 2012). *TRIP13* is also one of the top genes associated with chromosomal instability in human cancers (Carter et al., 2006). A reasonable surmise is that similar to p31^{comet} (Chan et al., 2008b), overexpression of TRIP13 may induce premature mitotic exit. In contrast, downregulation of TRIP13 may induce genome instability through delayed mitotic exit. The resulting increase in C-MAD2 may also compromise SAC activation during mitosis. Yet another speculation is that similar to our previous findings for p31^{comet} (Ma et al., 2012), the level of TRIP13 may affect the sensitivity of antimitotic drug treatments.

EXPERIMENTAL PROCEDURES

DNA Constructs
See Supplemental Experimental Procedures for constructs and details of subcloning.

Cell Culture
See Supplemental Experimental Procedures for details of cells used in this study, flow cytometry, and cell imaging.

Cell Cycle Synchronization
Cell cycle synchronization was performed as described (Ma and Poon, 2011a). Briefly, mitotic cells were obtained by incubating cells released from a double thymidine method with NOC before the mitotic cells were isolated with mechanical shake-off. In some cases, mitotic cells were washed twice with PBS and released into drug-free medium. Mitotic TRIP13-deficient cells were obtained by first synchronizing cells to G$_2$ using a double thymidine method followed by 4 hr of RO3306 treatment. The RO3306-treated cells were then released to drug-free medium for 30 min and before addition of MG132 for 1 hr. The cells were then further treated with NOC for 30 min to activate the SAC.

Antibodies and Immunological Methods
Monoclonal antibodies against β-actin, FLAG (Sigma-Aldrich), HA, CDC20, MAD1 (Santa Cruz Biotechnology), MAD2, BUB3, and CDC27 (BD Transduction Laboratories) were obtained from the indicated suppliers. Polyclonal antibodies against APC4 (Abcam), BUBR1, HA (Bethyl Laboratories), FLAG (Rockland Immunochemicals), phosphor-histone H3^{Ser10}, and TRIP13 (Santa Cruz Biotechnology) were obtained from the indicated suppliers. Antibodies against cyclin B1 were gifts from Julian Gannon (Cancer Research). Polyclonal antibodies against MAD2 (Ma and Poon, 2011b) and p31^{comet} (Ma et al., 2012) were prepared as previously described. Autoantibody against human nuclear ANA-centromere CREST was obtained from Fitzgerald Industries. Anti-FLAG (M2)-conjugated agarose for immunoprecipitation was obtained from Sigma-Aldrich. Immunoblotting was performed as previously described (Poon et al., 1995), except that a ChemiDoc Touch imaging system (Bio-Rad) was used to detect the signals. Immunoprecipitation and immunostaining of MAD2 were performed as described (Ma and Poon, 2011b).

MAD2 Conformation Analysis and Cell Lysate MAD2 Conversion Assays
MAD2 conformation was determined using spin column-based ion exchange chromatography. Spin columns with 100 μl of SOURCE 15Q matrix (GE Healthcare) were washed sequentially with 1 M NaCl, 1 M HCl, 500 mM NaOH and equilibrated with buffer A (5 mM Tris-HCl [pH 7.5], 25 mM NaCl, 0.5 mM EDTA, 5 mM NaF, 0.01% NP40). Cell lysates (400 μg) were diluted ten times with water before being loaded onto the column (100 μl). The lysate loaded columns were washed three times with buffer A and then step eluted with 150 μl buffer A containing 5%–22.5% of buffer B (5 mM Tris-HCl [pH 7.5], 1.025 M NaCl, 0.5 mM EDTA, 5 mM NaF, 0.01% NP40). The eluted fractions were mixed with SDS-sample buffer and analyzed using immunoblotting.

For MAD2 conversion assay, cell lysates (400 μg) were diluted 2-fold with water and supplemented with 1 mM ATP, 20 mM MgCl$_2$, 0.1 mg/ml creatine kinase, and 10 mM phosphocreatine. The lysates were incubated with purified GST-TRIP13 (1 μg) or cell lysates (40 μg) at 25°C for the indicated time. The reaction were stopped by 5-fold dilution with water and loaded onto the spin column to analyze the MAD2 conformation. GST-TRIP13 was expressed in bacteria and purified with GSH-agarose chromatography as described (Poon et al., 1995), except that 18°C was used for induction.

Statistical Analysis
Box-and-whisker plots (center lines show the medians; box limits indicate interquartile range; whiskers extend 1.5 times the interquartile range from the 25th and 75th percentiles) were generated by RStudio. Student's t test was used to calculate statistical significance (*p < 0.05; **p < 0.01; ***p < 0.001).
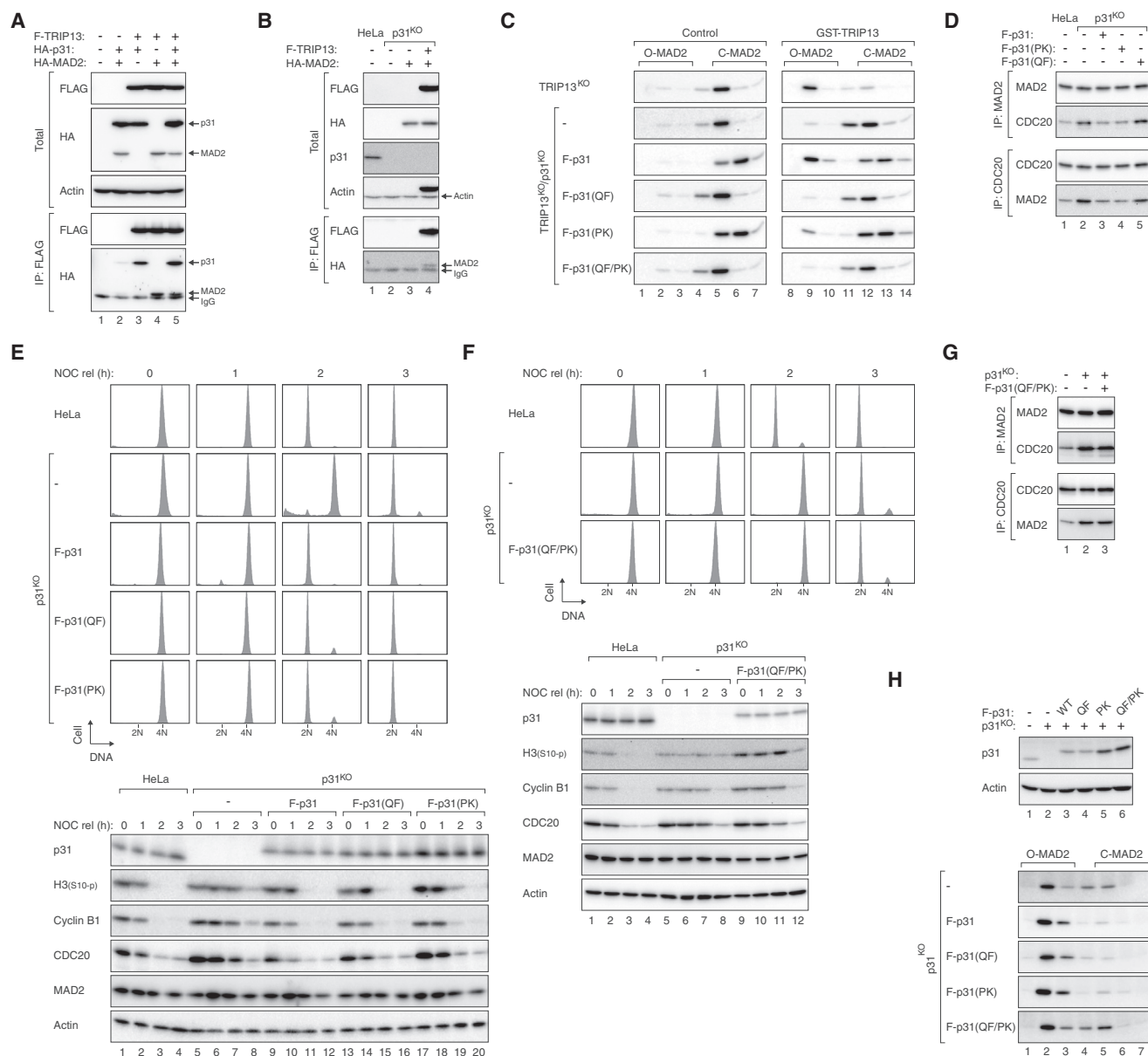
Figure 7. Interaction of p31comet with Either MAD2 or TRIP13 Can Promote Mitotic Exit

(A) TRIP13 forms a complex with p31comet and MAD2. FLAG-TRIP13, HA-p31comet, and HA-MAD2 were expressed in HeLa cells. Lysates were subjected to immunoprecipitation using an antibody against FLAG. Both the total lysates and the immunoprecipitates were analyzed with immunoblotting.

(B) TRIP13 can interact with MAD2 in the absence of p31comet. FLAG-TRIP13 and HA-MAD2 were expressed in p31KO. Lysates were subjected to immuno-precipitation using an antibody against FLAG. Both the total lysates and the immunoprecipitates were analyzed with immunoblotting. HeLa cells were also used as a control.

(C) Lysates of TRIP13KO or TRIP13KO/p31KO re-expressing different p31comet mutants were supplemented with an ATP-regeneration system and incubated with either buffer or bacterially expressed GST-TRIP13. After 60 min, the reactions were stopped, and MAD2 conformation was analyzed with ion exchange chromatography.

(D) Binding to MAD2 is critical for p31comet to inhibit MCC formation. The indicated FLAG-tagged p31comet constructs were introduced into p31KO. The cell lines were enriched in mitosis with NOC. Lysates were prepared and subjected to immunoprecipitation using antiserum against MAD2 or CDCD20. The immuno-precipitates and total lysates were then analyzed using immunoblotting.

(E) Binding to neither MAD2 nor TRIP13 is crucial for p31comet's function in mitotic exit. NOC was used to synchronize p31KO expressing different p31comet constructs in mitosis. The cells were then released into NOC-free medium and harvested for flow cytometry analysis at the indicated time points (upper). Lysates were also prepared and analyzed with immunoblotting (lower). HeLa cells were also used as a control.

(legend continued on next page)

REFERENCES

Banerjee, R., Russo, N., Liu, M., Basrur, V., Bellile, E., Palanisamy, N., Scanlon, C.S., van Tubergen, E., Inglehart, R.C., Metwally, T., et al. (2014). TRIP13 promotes error-prone nonhomologous end joining and induces chemoresistance in head and neck cancer. Nat. Commun. 5, 4527.

Carter, S.L., Eklund, A.C., Kohane, I.S., Harris, L.N., and Szallasi, Z. (2006). A signature of chromosomal instability inferred from gene expression profiles predicts clinical outcome in multiple human cancers. Nat. Genet. 38, 1043–1048.

Chan, Y.W., Ma, H.T., Wong, W., Ho, C.C., On, K.F., and Poon, R.Y. (2008a). CDK1 inhibitors antagonize the immediate apoptosis triggered by spindle disruption but promote apoptosis following the subsequent rereplication and abnormal mitosis. Cell Cycle 7, 1449–1461.

Chan, Y.W., On, K.F., Chan, W.M., Wong, W., Siu, H.O., Hau, P.M., and Poon, R.Y. (2008b). The kinetics of p53 activation versus cyclin E accumulation underlies the relationship between the spindle-assembly checkpoint and the postmitotic checkpoint. J. Biol. Chem. 283, 15716–15723.

De Antoni, A., Pearson, C.G., Cimini, D., Canman, J.C., Sala, V., Nezi, L., Mapelli, M., Sironi, L., Faretta, M., Salmon, E.D., and Musacchio, A. (2005). The Mad1/Mad2 complex as a template for Mad2 activation in the spindle assembly checkpoint. Curr. Biol. 15, 214–225.

Eytan, E., Wang, K., Miniowitz-Shemtov, S., Sitry-Shevah, D., Kaisari, S., Yen, T.J., Liu, S.T., and Hershko, A. (2014). Disassembly of mitotic checkpoint complexes by the joint action of the AAA-ATPase TRIP13 and p31(comet). Proc. Natl. Acad. Sci. USA 111, 12019–12024.

Habu, T., Kim, S.H., Weinstein, J., and Matsumoto, T. (2002). Identification of a MAD2-binding protein, CMT2, and its role in mitosis. EMBO J. 21, 6419–6428.

Hanson, P.I., and Whiteheart, S.W. (2005). AAA+ proteins: have engine, will work. Nat. Rev. Mol. Cell Biol. 6, 519–529.

Larkin, S.E., Holmes, S., Cree, I.A., Walker, T., Basketter, V., Bickers, B., Harris, S., Garbis, S.D., Townsend, P.A., and Aukim-Hastie, C. (2012). Identification of markers of prostate cancer progression using candidate gene expression. Br. J. Cancer 106, 157–165.

Li, X.C., and Schimenti, J.C. (2007). Mouse pachytene checkpoint 2 (trip13) is required for completing meiotic recombination but not synapsis. PLoS Genet. 3, e130.

Luo, X., Tang, Z., Xia, G., Wassmann, K., Matsumoto, T., Rizo, J., and Yu, H. (2004). The Mad2 spindle checkpoint protein has two distinct natively folded states. Nat. Struct. Mol. Biol. 11, 338–345.

Ma, H.T., and Poon, R.Y. (2011a). Synchronization of HeLa cells. Methods Mol. Biol. 761, 151–161.

Ma, H.T., and Poon, R.Y. (2011b). Orderly inactivation of the key checkpoint protein mitotic arrest deficient 2 (MAD2) during mitotic progression. J. Biol. Chem. 286, 13052–13059.

Ma, H.T., Chan, Y.Y., Chen, X., On, K.F., and Poon, R.Y. (2012). Depletion of p31comet protein promotes sensitivity to antimitotic drugs. J. Biol. Chem. 287, 21561–21569.

Mapelli, M., Massimiliano, L., Santaguida, S., and Musacchio, A. (2007). The Mad2 conformational dimer: structure and implications for the spindle assembly checkpoint. Cell 131, 730–743.

Musacchio, A. (2015). The Molecular Biology of Spindle Assembly Checkpoint Signaling Dynamics. Curr. Biol. 25, R1002–R1018.

Nelson, C.R., Hwang, T., Chen, P.H., and Bhalla, N. (2015). TRIP13PCH-2 promotes Mad2 localization to unattached kinetochores in the spindle checkpoint response. J. Cell Biol. 211, 503–516.

Pesin, J.A., and Orr-Weaver, T.L. (2008). Regulation of APC/C activators in mitosis and meiosis. Annu. Rev. Cell Dev. Biol. 24, 475–499.

Poon, R.Y., Toyoshima, H., and Hunter, T. (1995). Redistribution of the CDK inhibitor p27 between different cyclin.CDK complexes in the mouse fibroblast cell cycle and in cells arrested with lovastatin or ultraviolet irradiation. Mol. Biol. Cell 6, 1197–1213.

Rhodes, D.R., Yu, J., Shanker, K., Deshpande, N., Varambally, R., Ghosh, D., Barrette, T., Pandey, A., and Chinnaiyan, A.M. (2004). Large-scale meta-analysis of cancer microarray data identifies common transcriptional profiles of neoplastic transformation and progression. Proc. Natl. Acad. Sci. USA 101, 9309–9314.

Vader, G. (2015). Pch2(TRIP13): controlling cell division through regulation of HORMA domains. Chromosoma 124, 333–339.

van Kester, M.S., Borg, M.K., Zoutman, W.H., Out-Luiting, J.J., Jansen, P.M., Dreef, E.J., Vermeer, M.H., van Doorn, R., Willemze, R., and Tensen, C.P. (2012). A meta-analysis of gene expression data identifies a molecular signature characteristic for tumor-stage mycosis fungoides. J. Invest. Dermatol. 132, 2050–2059.

Wang, K., Sturt-Gillespie, B., Hittle, J.C., Macdonald, D., Chan, G.K., Yen, T.J., and Liu, S.T. (2014). Thyroid hormone receptor interacting protein 13 (TRIP13) AAA-ATPase is a novel mitotic checkpoint-silencing protein. J. Biol. Chem. 289, 23928–23937.

Westhorpe, F.G., Tighe, A., Lara-Gonzalez, P., and Taylor, S.S. (2011). p31comet-mediated extraction of Mad2 from the MCC promotes efficient mitotic exit. J. Cell Sci. 124, 3905–3916.

(F) Disruption of both MAD2 and TRIP13 binding abolishes p31[comet]'s function in mitotic exit. NOC was used to synchronize p31[KO] or p31[KO] expressing p31(QF/PK) in mitosis. The cells were then released into NOC-free medium and harvested for flow cytometry analysis at the indicated time points (upper). Lysates were also prepared and analyzed with immunoblotting (lower). HeLa cells were also used as a control.

(G) Disruption of both MAD2 and TRIP13 binding abolishes p31[comet]'s function in inhibiting MCC formation. NOC was added to enrich p31[KO] or p31[KO] expressing p31(QF/PK) in mitosis. Lysates were prepared and subjected to immunoprecipitation using antiserum against MAD2 or CDCD20. The immunoprecipitates and total lysates were then analyzed using immunoblotting.

(H) Either MAD2 or TRIP13 binding is sufficient for p31[comet] to induce C-MAD2 to O-MAD2 conversion. The indicated FLAG-p31[comet] constructs were transiently transfected into p31[KO]. Lysates were prepared and MAD2 conformation was analyzed with ion exchange chromatography. The relative expression of endogenous p31[comet] and the various p31[comet] constructs is shown at the top.

Xia, G., Luo, X., Habu, T., Rizo, J., Matsumoto, T., and Yu, H. (2004). Conformation-specific binding of p31(comet) antagonizes the function of Mad2 in the spindle checkpoint. EMBO J. *23*, 3133–3143.

Yang, M., Li, B., Tomchick, D.R., Machius, M., Rizo, J., Yu, H., and Luo, X. (2007). p31comet blocks Mad2 activation through structural mimicry. Cell *131*, 744–755.

Ye, Q., Rosenberg, S.C., Moeller, A., Speir, J.A., Su, T.Y., and Corbett, K.D. (2015). TRIP13 is a protein-remodeling AAA+ ATPase that catalyzes MAD2 conformation switching. eLife *4*.

Yu, H. (2006). Structural activation of Mad2 in the mitotic spindle checkpoint: the two-state Mad2 model versus the Mad2 template model. J. Cell Biol. *173*, 153–157.